International Journal of Pharmaceutics: X 8 (2024) 100278

Contents lists available at ScienceDirect

International Journal of Pharmaceutics: X

journal homepage: www.sciencedirect.com/journal/international-journal-of-pharmaceutics-x

Platelet Membrane-Encapsulated Poly(lactic-*co*-glycolic acid) Nanoparticles Loaded with Sildenafil for Targeted Therapy of Vein Graft Intimal Hyperplasia

Fajing Yang [a,c,1], Yihui Qiu [a,1], Xueting Xie [a,c], Xingjian Zhou [c], Shunfu Wang [c], Jialu Weng [c], Lina Wu [c], Yizhe Ma [a], Ziyue Wang [a], Wenzhang Jin [b,c,*], Bicheng Chen [a,c,*]

[a] *Department of Vascular Surgery, The First Affiliated Hospital of Wenzhou Medical University, Wenzhou, Zhejiang Province 325000, PR China*
[b] *Department of Colorectal Surgery, The Second Affiliated Hospital of Zhejiang Chinese Medical University, Hangzhou 310000, PR China*
[c] *Key Laboratory of Diagnosis and Treatment of Severe Hepato-Pancreatic Diseases of Zhejiang Province, The First Affiliated Hospital of Wenzhou Medical University, Wenzhou 325000, PR China*

ARTICLE INFO

Keywords:
Platelet membrane
Sildenafil
PLGA
Vein graft
Intimal hyperplasia

ABSTRACT

Autologous vein grafts have attracted widespread attention for their high transplantation success rate and low risk of immune rejection. However, this technique is limited by the postoperative neointimal hyperplasia, recurrent stenosis and vein graft occlusion. Hence, we propose the platelet membrane-coated Poly(lactic-*co*-glycolic acid) (PLGA) containing sildenafil (PPS). Platelet membrane (PM) is characterised by actively targeting damaged blood vessels. The PPS can effectively target the vein grafts and then slowly release sildenafil to treat intimal hyperplasia in the vein grafts, thereby preventing the progression of vein graft restenosis. PPS effectively inhibits the proliferation and migration of vascular smooth muscle cell (VSMCs) and promotes the migration and vascularisation of human umbilical vein endothelial cells (HUVECs). In a New Zealand rabbit model of intimal hyperplasia in vein grafts, the PPS significantly suppressed vascular stenosis and intimal hyperplasia at 14 and 28 days after surgery. Thus, PPS represents a nanomedicine with therapeutic potential for treating intimal hyperplasia of vein grafts.

1. Introduction

Atherosclerotic occlusive diseases, such as lower extremity arterial occlusive disease and coronary artery atherosclerotic heart disease, are becoming increasingly prevalent and significantly impact individual health and quality of life (Charakida and Tousoulis, 2013; Cole, 2017; Shishehbor and Jaff, 2016). Arterial bypass surgery is a crucial therapeutic approach for these conditions, with autologous vein grafts being the preferred choice (Beerkens et al., 2022). Nevertheless, vein grafts may lead to recurrent stenosis, affecting long-term treatment outcomes (Neufang et al., 2018; Royse et al., 2022). The recurrence of stenosis and occlusion in vein grafts associated with to early thrombus formation, mid-to-late-stage neointimal hyperplasia and the development of atherosclerosis (Yao et al., 2014). Mid-to-late-stage intimal hyperplasia is the main contributor to vein graft failure (Tang et al., 2022). Surgical procedures for vein graft liberation, ligation, division, transplantation and vascular bypass reperfusion cause varying degrees of endothelial damage, accompanied by the accumulation of platelets and neutrophils as well as release of cytokines and chemokines (Dashwood et al., 2007; Ladak et al., 2022; Ward et al., 2017). This process leads to hyperproliferation of smooth muscle cells, resulting in intimal hyperplasia and restenosis of vein grafts (Qi et al., 2017). Currently, postoperative restenosis of vein grafts has attracted clinical attention, yet effective therapeutic approaches remain elusive.

Phosphodiesterase-5 (PDE-5) inhibitors, such as sildenafil and tadalafil, represent a significant class of cardiovascular therapeutic agents (Nilsson et al., 2023). Clinically, they are utilized to treat disorders such as erectile dysfunction, pulmonary arterial hypertension (PAH) and heart failure (Guazzi, 2008; Hamzehnejadi et al., 2022; Lan et al., 2018). The mechanism of PDE-5 inhibitors is related to nitric

* Corresponding authors at: Key Laboratory of Diagnosis and Treatment of Severe Hepato-Pancreatic Diseases of Zhejiang Province, The First Affiliated Hospital of Wenzhou Medical University, Wenzhou 325000, PR China.
E-mail addresses: 228927178@qq.com (W. Jin), chenbicheng@hotmail.com (B. Chen).
[1] These authors contributed equally to this work.

https://doi.org/10.1016/j.ijpx.2024.100278
Received 23 April 2024; Received in revised form 9 August 2024; Accepted 15 August 2024
Available online 17 August 2024

oxide (NO) and mainly acts through the nitric oxide-cyclic guanosine monophosphate (NO-cGMP) signaling pathway (Mo et al., 2004). NO is known for its vasodilatory property, antiplatelet aggregation, anti-oxidative stress, anti-inflammation, anti-proliferation and pro-fibrinolytic effects (Lordan et al., 2021). PDE-5 inhibitors, a potential therapy for postoperative vein graft stenosis, attenuate intimal hyperplasia in vein grafts by modulating the NO-cGMP signaling pathway and inhibiting smooth muscle cell migration and proliferation (Degjoni et al., 2022; Reffelmann and Kloner, 2003). At present, sildenafil has been approved for the treatment of PAH in adult patients (Vizza et al., 2017). Previous studies have indicated that sildenafil exerts positive effects on inhibiting intimal hyperplasia, suggesting it might be an ideal drug for reducing vein graft restenosis.

Poly(lactic-*co*-glycolic acid) (PLGA) nanoparticles are widely used in pharmaceutical delivery systems due to their excellent biocompatibility and controlled release properties (Mohebali and Abdouss, 2020). Encapsulation of sildenafil into PLGA nanoparticles offers several advantages. Firstly, it improves the solubility and stability of the drug, thereby enhancing its bioavailability. Secondly, the controlled release of sildenafil from PLGA nanoparticles can lead to sustained drug levels in the bloodstream, thereby reducing the frequency of dosing and minimizing side effects (Liang et al., 2024; Stipa et al., 2021). Current studies of sildenafil-loaded PLGA nanoparticles have focused on pulmonary disease (e.g. PAH), and most of the loading methods used are emulsified solvent volatilisation. These studies have shown promising results in terms of enhanced delivery, sustained release and improved therapeutic efficacy of PLGA nanoparticles containing sildenafil (Lazo et al., 2023; Rashid et al., 2017; Restani et al., 2020; Shahin et al., 2021). It has been shown that PLGA nanoparticles loaded with sildenafil have significantly higher bioavailability, longer circulation time and outstanding therapeutic effects in PAH compared to free sildenafil (Rashid et al., 2017). In conclusion, PLGA nanoparticles containing sildenafil display great potential for improving drug delivery and efficacy.

Effective delivery of drug-loaded nanoparticles to the injury site is conducive to reducing the side effects of the drug and enhancing their therapeutic efficacy (Zhang et al., 2023). Platelets play a pivotal sentinel role in monitoring vascular damage and defending against invasive microorganisms, which inspire the innovative design of functional nanocarriers (Holinstat and Reviews, 2017; Hu et al., 2015). The mechanisms of platelet aggregation, and in particular their ability in response to vascular impairment, have contributed to the development of a platelet mimetic delivery system capable of showing significant targeted therapeutic potential in the areas of vascular repair, inflammation response, and cancer treatment (Kulkarni et al., 2000). Platelet membrane (PM)-coated nanoparticles exhibit exceptional biocompatibility, which can mimic cellular functions, evade immune system detection, and specifically deliver drug-loaded nanoparticles to the desired location, thereby achieving targeted therapeutic objectives and enhancing treatment efficacy (Hu et al., 2015; Xu et al., 2023). Especially for patients after vein graft surgery, these PM-coated nanoparticles are considered an ideal choice for targeted drug delivery to damaged vessels thanks to their strong specificity.

Collectively, it is hypothesised that sildenafil may exert therapeutic effects in preventing restenosis after vein graft surgery by inhibiting intimal hyperplasia. Therefore, the aim and novelty of this study is to develop for the first time a platelet membrane-encapsulated PLGA nanoparticle containing sildenafil for the treatment of vascular stenosis due to intimal hyperplasia after vein grafting. As a drug carrier, PLGA can prolong the duration of the drug efficiency. Encapsulation with PM enhances drug uptake by damaged blood vessels, significantly improving target delivery and therapeutic efficacy in vascular injury.

In this work, we chose sildenafil as the therapeutic drug, loaded sildenafil onto PLGA by nanoprecipitation (SNP) and covered platelets on the surface of SPN by extruder to obtain platelet membrane-encapsulated PLGA nanoparticles containing sildenafil (PPS). The PPS demonstrated targeting capability towards vein grafts, allowing for the slow release of sildenafil in the body to exert its therapeutic effects. Results from in vitro and in vivo animal studies indicated that the PPS assisted in avoiding vascular stenosis, promoting endothelial repair, inhibiting intimal hyperplasia and inflammatory responses.

2. Materials and methods

2.1. Materials

Poly (lactic-*co*-glycolic acid) (PLGA) (lactide:glycolide 50:50, 10,000–15,000 Da, Xfnano, 103,390, Nanjin,China), Sildenafil citrate (Aladdin, A2329533, Shanghai, China), Poloxamer 188 (Sigma, P5556, Shanghai, China), Acetone (Sigma, 904,082, Shanghai, China), Rabbit Peripheral Blood Platelet Separation Reagent Kit (Solarbio, P1730, Beijing, China), BSA-FITC(qiyuebio, Q-0176281, Xian, China), Enhanced Cell Counting Kit-8 (CCK-8, Beyotime, C0042, Shanghai, China), 1,1'-Dioctadecyl-3,3,3′,3'-Tetramethylindodicarbocyanine,4-Chlorobenzenesulfonate Salt (DiD, Beyotime, C1039, Shanghai, China), Calcein-AM/PI Staining Kit (Beyotime, C2015M, Shanghai, China), Anti-CD68 antibody (ab125212), Anti-alpha Smooth Muscle Actin (α-SMA) antibody (ab7817) and Anti-CD31 antibody (ab182921,) were purchased from Abcam (Shanghai, China), Rabbit Proliferating Cell Nuclear Antigen (PCNA) ELISA kit (Tzybiotech, TK06247, Wuhan, China), Rabbit vascular endothelial growth factor (VEGF) ELISA KIT (SEKRT-0009), Rabbit platelet-derived growth factor (PDGF) ELISA KIT (SEKRT-0400) and Rabbit TNF-α ELISA Kit (SEKRT-0009), Rabbit IL-1β ELISA Kit (SEKRT-0019) were purchased from Solarbio (Beijing, China). DMEM medium, fetal bovine serum (FBS) and phosphate buffered saline (PBS) were purchased from the Bionove-gene Biomedical Technology Co., Ltd. (Shanghai, China). Pentobarbital sodium, heparin and saline were provided by the Experimental Animal Centre of Wenzhou Medical University. All other chemicals were reagent grade and used as received. HUVECs and VSMCs purchased from the BHcell Biotechnology Co., Ltd. (Guangzhou, China).

2.2. Methods

2.2.1. Synthesis of PLGA loaded with sildenafil

Nanoprecipitation method was employed to prepare sildenafil-loaded PLGA nanoparticles (Hu et al., 2015; Wei et al., 2018; Zhao et al., 2021). Briefly, a solution containing PLGA (10 mg) and sildenafil (4 mg) in acetone (1 mL) was added dropwise to an aqueous solution containing 0.05% (wt/vol) poloxamer 188 (5 mL). The mixture was stirred for 6 h and the residual acetone was further removed by rotary evaporation. The unencapsulated drug was separated from the nanoparticles by centrifugation at 3000× *g* for 30 min using a ultrafiltration tube (molecular weight cut-off at 10000 Da, Cobetter). The separated nanoparticles were resuspended by adding appropriate amount of pure water. The resuspended solution was collected and lyophilized in a freeze-dryer to obtain sildenafil-loaded PLGA nanoparticles (SPN).

The excess unencapsulated sildenafil was separated and The concentration of free sildenafil was then obtained by measuring the absorbance at 290 nm using high performance liquid chromatography (HPLC) (Jung et al., 2011; Salama et al., 2016). The amount of sildenafil loaded in the SPN nanoparticles was quantified according to the following equation:

Amount of sildenafil contained in nanoparticles $= C_0 \times V_0 - C_1 \times V_1$

C_0: concentration of sildenafil at the start of the reaction; V_0: volume of solution at start of reaction; C_1: concentration of sildenafil at the end of the reaction; V_1: volume of solution at end of reaction.

The drug loading efficiency and drug-loading were calculated according to the following formulae:

Loading efficiency $= (1 - \text{Amount of unencapsulated sildenafil/Total amount of sildenafil added}) \times 100\%$.

Drug − loading $=$ Amount of sildenafil contained in nanoparticles/Total weight of nanoparticles $\times 100\%$.

Record the PPS containing 1 mg of sildenafil as 1 unit.

2.2.2. Platelet isolation and platelet membrane derivation

Suitable adult male New Zealand rabbits were selected and blood was collected through marginal ear vein using citrate buffer as an anticoagulant. According to the instructions provided in the rabbit peripheral blood platelet separation kit (Solarbio, P1730, China), platelets were isolated. Briefly, dilute fresh anticoagulated whole blood with equal volumes of PBS. In the centrifuge tube, 4 mL of isolation solution was added first, followed by 2 mL of 60% isolation solution (1200 μL isolation solution +800 μL tissue dilution solution, the kit provides both reagents), and then finally add the diluted whole blood (note: the total volume of the mixture should not exceed two-thirds of the centrifuge tube, or else the separation will be influenced). The mixture was centrifuged (300 *g*, 25 min) at room temperature. After centrifugation, the mixture was divided into 6 layers from top to bottom, and the platelet layer (second layer) was carefully pipetted into a clean centrifuge tube, then 10 mL PBS was added and centrifuged (500 *g*, 20 min), the supernatant was discarded. Platelets were obtained, resuspended in an adequate volume of PBS and subjected to repeated freeze-thaw cycles to extract platelet membranes (PM). The platelets were frozen at −80 °C and then thawed at room temperature, followed by centrifugation at 4000 ×*g* for 3 min. The platelet suspension was frozen and thawed at least three times (Hu et al., 2015). Finally, the PM was resuspended in PBS.

2.2.3. Platelet membrane-coated SPN

PM were sonicated at a frequency of 40 kHz and 100 W power for 5 min in a covered EP tube. The resulting suspension was sequentially extruded through 400 nm and 200 nm porous polycarbonate membranes using an Avanti mini-extruder (Avanti Polar Lipids, AL, USA) in 10 cycles to obtain PM-coated SPN (PPS). PM extracted from 1 mL of rabbit blood was extruded with PLGA containing 1 mg of sildenafil in a 1:1 ratio by solution volume (Xiao et al., 2022). Specifically, 1 mL of 35.3 μg/mL PM was extruded with 1 mL of 1.60 mg/mL SPN through a film extruder so that the PM coated the SPN. Empty platelet membrane vesicles were prepared by a similar method.

2.2.4. Characterization of the nanoparticles

The morphology of nanoparticles was observed by transmission electron microscope (TEM, Hitachi, HT7800, Japan). Before performing TEM imaging, the samples were prepared by depositing the nanoparticle suspension on a 200-mesh copper grid and then negatively stained with freshly prepared 1 wt% uranyl acetate. The size distribution and zeta potential of nanoparticles were determined using dynamic light scattering (DLS, Zetasizer Nano-ZS, Malvern, UK) ($n = 3$ per group). The absorption spectrum of nanoparticles was recorded using a UV–Visible spectrophotometer (Cary 60, China).

2.2.5. In vitro release experiment

Using the same procedure as described above, 1 mg of sildenafil loaded nanoparticles were added to 2 mL PBS at 37 °C and gently shaken. At predetermined time points, the above solution was centrifuged (5000 rpm, 10 min) and 50 μL of supernatant was collected Determination of Sildenafil Content in the Collected Supernatant by HPLC. Finally, the in vitro release of sildenafil was calculated based on sildenafil content in supernatant ($n = 3$ per group).

2.2.6. Cytotoxicity assay

Human umbilical vein endothelial cells (HUVECs) were cultured in a humidified cell culture incubator with 5% carbon dioxide at 37 °C. Cells were cultured in DMEM medium (Gibco, USA) supplemented with 10% (*v*/v) fetal bovine serum (FBS) (Gibco, USA). The cytotoxicity of the PPS was tested in HUVECs via an CCK-8 assay. HUVECs were seeded in 96-well plates with a density of 5×10^4 cells per well. After cell attachment, the cells were treated with DMEM medium with or without PPS (1 unit) and incubated in a cell culture incubator for 12 and 48 h. After washing with PBS, medium (200 μL) containing 20 μL of CCK-8 was added to each well and incubated at 37 °C for 4 h. The absorbance of each well at 450 nm was measured with enzyme markers and cell activity was calculated ($n = 5$ per group). In 48 h, according to the manufacturer's instructions, HUVECs were stained with calcein-AM/PI staining kit. The fluorescence images were captured by a fluorescence microscope.

2.2.7. Cell scratch experiment

When the HUVECs and vascular smooth muscle cells (VSMCs) density approximately reached 100% in 6-well plates, and then the cell monolayers were scratched using a 200 μL pipette tip. Cells were then incubated in serum-free DMEM with sildenafil (1 mg/mL) or PPS (1unit) for 12 and 48 h. Cell migration was recorded microscopically and the width of the scratch at each time point was analyzed using image J to calculate the cell migration rate ($n = 3$ per group).

Migration rate $=$ (Initial distance − migration distance)/Initial distance $\times 100\%$.

2.2.8. Tube formation experiment

Fifty μL of Matrigel (Corning, USA) was applied to a 24-well plate in an even distribution to avoid air bubbles and incubated at 37 °C for 30 min or polymerized for 1 h at room temperature. 500 μL of HUVECs cell suspension was seeded at a density of 1×10^5 cells per well. Cells were treated with medium containing sildenafil (1 mg/mL) or PPS (1unit) or neither. Staining of HUVECs cell using calcein-AM. The formation of HUVECs forming tubes was observed for 8 h using a microscope (Nikon,

Japan). Finally, the number of tube-forming cells in each group was counted ($n = 3$ per group).

2.2.9. Cell proliferation assay

VSMCs were inoculated into 96-well plates at a density of approximately 3×10^3/well. Old medium was aspirated after cell apposition and the cells were washed 3 times with PBS, after which they were treated with medium containing sildenafil (1 mg/mL) or PPS (1 unit) or neither, and incubated for 48 h. The cells were washed with PBS 3 times and then 200 μL of serum-free medium containing 20 μL of CCK-8 solution were added to each well and then the cells were incubated for 1 h. After incubation, the absorbance was measured at 450 nm. Finally, the cell proliferation rate was calculated ($n = 3$ per group).

$$\text{Proliferation rate} = \text{Absorbance at 48 h} / \text{Initial moment of absorbance} \times 100\%.$$

2.2.10. Hemolysisi assay

Blood from healthy adult New Zealand rabbits were taken through marginal ear veins and placed into tubes containing sodium citrate anticoagulant. The blood samples were gently centrifuged (1500 rpm, 10 min) to remove the supernatant and the remaining precipitated erythrocytes were washed with an appropriate amount of saline and then centrifuged as described above until the supernatant did not show any red color. The resulting erythrocytes were prepared as a 2% erythrocyte suspension in saline. Four EP tubes with 1 mL of 2% erythrocyte suspension were taken and then 100 μL of saline was added as negative control group, 1% Triton X-100 as positive control group,1 mg/mL sildenafil and 1 unit of PPS as two experimental groups, respectively, and then placed them in a 37 °C water bath for 8 h. After gentle centrifugation (1500 rpm for 10 min), the EP tube supernatant color was observed and photographed. Then 100 μL of supernatant was carefully pipetted into a 96-well plate and the absorbance was detected at 540 nm via an enzyme marker ($n = 5$ per group).

$$\text{Hemolysis rate} = (\text{absorbance of sample} - \text{absorbance of negative control}) / (\text{absorbance of positive control} - \text{absorbance of negative control}) \times 100\%.$$

$$\text{Vascular stenosis rate} = \text{vessel diameter at the time of testing} / \text{initial vessel diameter} \times 100\%.$$

2.2.11. Vein graft animal model

In this study, general grade New Zealand rabbits, weighing between 3.0–3.5 kg, were selected from the Animal Experiment Centre of Wenzhou Medical University. All rabbits were housed in rabbit cages in the general grade animal room of the Animal Experiment Centre of Wenzhou Medical University. Animals are housed in the facility at an indoor temperature of about 18–25 °C with a daily temperature difference of ± 5 °C and humidity levels maintained at 50% at cage level. Animals were housed under a 12 h–12 h light–dark cycle and food and water were provided ad libitum. Animal maintenance and procedures were performed in accordance with the Ethics Committee of Wenzhou Medical University and the Experimental Animal Management Committee of Zhejiang Province (Approval No.: wydw2023–0233).

The New Zealand rabbit autologous vein graft model was established using the "cuff" method. The rabbit external jugular vein was grafted to the ipsilateral common carotid artery (Bongaarts et al., 2020; Wong et al., 2008; Wu et al., 2018). The surgical procedure was as follows: rabbits were anesthetized using 3% sodium pentobarbital (1 mL/kg) intravenously through the ear margins, with an additional intraoperative anaesthetic dose added at 1/10 to 1/6 of the anaesthetic dose if the operation lasted longer than 50 min. New Zealand rabbits were placed supine on a rabbit operating table, while their necks were exposed routinely prepared, disinfected and covered with a sterile cavity towel. In the midline of the rabbit's neck, between the sternum and the mandible, the skin and subcutaneous tissue were dissected in layers to expose and separate the external jugular vein. A segment of the vein was harvested as the graft vein and saline solution containing 6000 U/L of heparin was used to flush out residual blood in the cavity to prevent thrombus formation. Simultaneously, heparin saline solution (200 U/kg) was injected into the marginal vein of the ear for systemic heparinization. A homemade cannula was made using a 4F catheter sheath (Terumo), which was secured at both ends of the graft vein and immersed in heparin saline after fabrication. Next, further dissection of the subcutaneous connective tissue was performed until the carotid artery was exposed. The blood flow at both ends of the carotid artery was occluded using atraumatic artery clamps. With a sharp blade, the carotid artery wall was gently incised and the prepared graft vein was inserted into both ends of the carotid artery. The inserted catheter was securely fixed with sutures to prevent slippage. Successful placement of the catheter was confirmed upon observing a strong pulsation.

The first day of surgery was recorded as 1 day, and the New Zealand rabbits were kept until 28 days after surgery. Sixteen rabbits were divided into four groups: the blank group underwent sham operation, the sildenafil group injected with sildenafil (1 mg/kg), the PPS group injected with PPS (1 unit/kg) and the control group injected with an equivalent volume of saline solution. Postoperatively, injections were administered via the marginal vein of the rabbit's ear every Monday and Thursday.

2.2.12. Vascular ultrasound

Rabbits were anesthetized with 3% sodium pentobarbital (1 mL/kg) solution and immobilized on a dissecting table. The fur on the neck area of the rabbits was removed using a shaver followed by an adequate amount of coupling agent was applied to enhance image visualization. The ultrasonographic images of the grafted vessels in each group of rabbits were recorded using a portable color ultrasound machine (SonoSite, M-Turbo). Changes in the vessel diameter and blood flow signals were observed and documented ($n = 3$ per group).

2.2.13. HE and Masson staining

Following the completion of treatment at different time points, the rabbits in each group were euthanised. Vascular tissues and major organs (heart, liver, spleen, lungs and kidneys) were excised, fixed in routine 4% paraformaldehyde solution, embedded in paraffin and sectioned. Subsequently, staining was conducted with hematoxylin and eosin (HE) and masson trichrome stain for further observation by an optical microscope. The slices were quantitatively analyzed using Image J software ($n = 3$ per group).

2.2.14. In vivo imaging targeting assey

The cell membrane dye DiD-labelled PPS was prepared for in vivo targeting experiments. Specifically, DiD dye (10 μM) was mixed with PPS (1 unit/kg) and incubated for 6 h at 4 °C in a light-proof shaker, followed by dialysis in PBS solution for 12 h to remove excess free DiD dye. After intravenous administration of the DiD-labelled PPS, in vivo tracking of PPS was conducted using an in vivo imaging system (IVIS

Spectrum, PerkinElmer, USA). Rabbits were euthanised at a predetermined time, and the major organs (heart, liver, spleen, lungs and kidneys) along with the grafted vessels as well as the contralateral normal vessels were collected for imaging. The fluorescence intensity of major organs and vessels was counted and analyzed ($n = 3$ per group).

2.2.15. In vivo pharmacokinetic release assay

Sildenafil (1 mg/kg) or PPS (1 unit/kg) was administered via the marginal ear vein. At a predetermined time point, at least 1 mL of blood sample was withdrawn from the marginal ear vein of the rabbits and added to the tubes containing heparin ($n = 3$ per group). The blood sample was centrifuged and a clear plasma layer was separated. 100 μL plasma was thoroughly mixed with 50 μL of borax(0.1 N), 1 mL of ether and 50 μL of nifedipine in acetonitrile solution (200 μg/mL) as an internal standard. The mixture was vortexed for 3 min and centrifuged (10,000 ×*g*, 10 min) to precipitate the proteins. The residue was redissolved in the mobile phase. The resulting solution (20 μL) was analyzed by HPLC (Agilent, USA) equipped with a Phenomenex Gemini-NX 5u C18 analytical column (0.5 μm, 25 cm × 0.46 cm, Phenomenex, USA). The mobile phase consisted of 20 mM KH_2PO_4 and acetonitrile (70:30, *v*/v). The eluent was monitored at a flow rate of 1.0 mL/min at 290 nm. The release of sildenafil was then calculated from the standard curve (Al-Hroub et al., 2016; Dahshan et al., 2019; Jung et al., 2011).

2.2.16. Immunohistochemical staining

After 4 and 12 weeks, the rabbit blood vessel samples, were subjected to routine immunohistochemical steps including 4% paraformaldehyde fixation, antigen detection, antibody conjugation and chromogenic visualization. The following primary antibodies were used: anti-CD68 (1:500), α-SMA (1:500) and anti-CD31 (1:500). Photographs of representative fields were taken using an optical microscope and positive areas in each image were quantified using Image J ($n = 3$ per group).

2.2.17. Enzyme linked immunosorbent assay (ELISA)

Vascular tissue samples were collected from each group and filter paper was used to absorb the surface moisture. Equal amounts of vascular tissue was then excised from each group and thoroughly disrupted using a high-throughput tissue grinder (SCIENTZ-48 L, China). For each 1 mg of tissue 10 μL of RIPA lysing solution was added, and the mixture was lysed for 10 min on ice, followed by centrifuged (10,000 *g*, 5 min). The supernatant was taken and the concentrations of PCNA, CD34, VEGF, PDGF, TNF-α and IL-β in the supernatant were detected according to the manufacturer's instructions using the appropriate ELISA kit ($n = 3$ per group).

2.2.18. Statistical analysis

Experiments were carried out at least three times for statistical analysis , and the results were expressed as mean ± standard deviation. Statistical significance was assessed using one-way ANOVA. In this study, $*p < 0.05$, $**p < 0.01$, $***p < 0.001$ and they were considered statistically significant.

3. Results and discussion

3.1. Preparation and characterization of PPS

The PPS nanoparticles targeting vein grafts were prepared by nanoprecipitation and extrusion encapsulation methods (Fig. 1). Initially, sildenafil and a small amount of poloxamer were encapsulated onto PLGA nanoparticles (SPN) through a nanoprecipitation method, and subsequently, platelet membranes (PM) were coated onto the surface of SPN via the extrusion process, ultimately forming the PPS. In order to verify that PM were successfully encapsulated on the surface of SPN, the morphology of the bare PLGA, SPN and PPS were characterised using TEM, showing the core-shell structure of synthesized PPS with platelet membranes fully enveloping them (Fig. 2A). Additionally, empty platelet membrane vesicles were also characterised by TEM (Fig. S1A). The changes in the particle size and zeta potential of the nanoparticles during synthesis process were measured using Dynamic Light Scattering (DLS) (Fig. 2B). The original PLGA had a particle size of 88.47 ± 1.60 nm and a zeta potential of −40.46 ± 2.06 mV. After drug loading, the PLGA particle size increased to 105.66 ± 3.21 nm and the potential decreased to −35.36 ± 0.97 mV, indicating successful incorporation of sildenafil into PLGA. Following thorough extrusion of the PM with SPN, the nanoparticle diameter further increased to 122.67 ± 4.04 nm and the zeta potential was further decreased to - 30.53 ± 1.46 mV, similar to the zeta potential of PM vesicles (−30.27 ± 0.80 mV), suggesting a complete coverage of SPN by the PM. The nanoparticles were

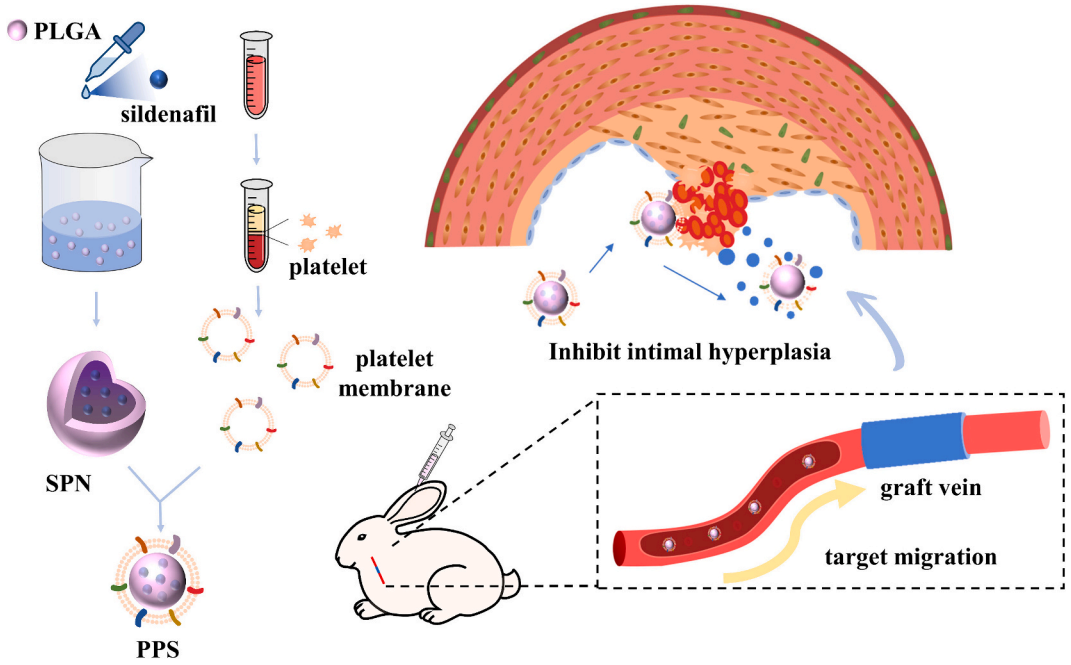

Fig. 1. Schematic diagram of PPS synthesis and its therapeutic process in the treatment of intimal hyperplasia in rabbit vein graft.

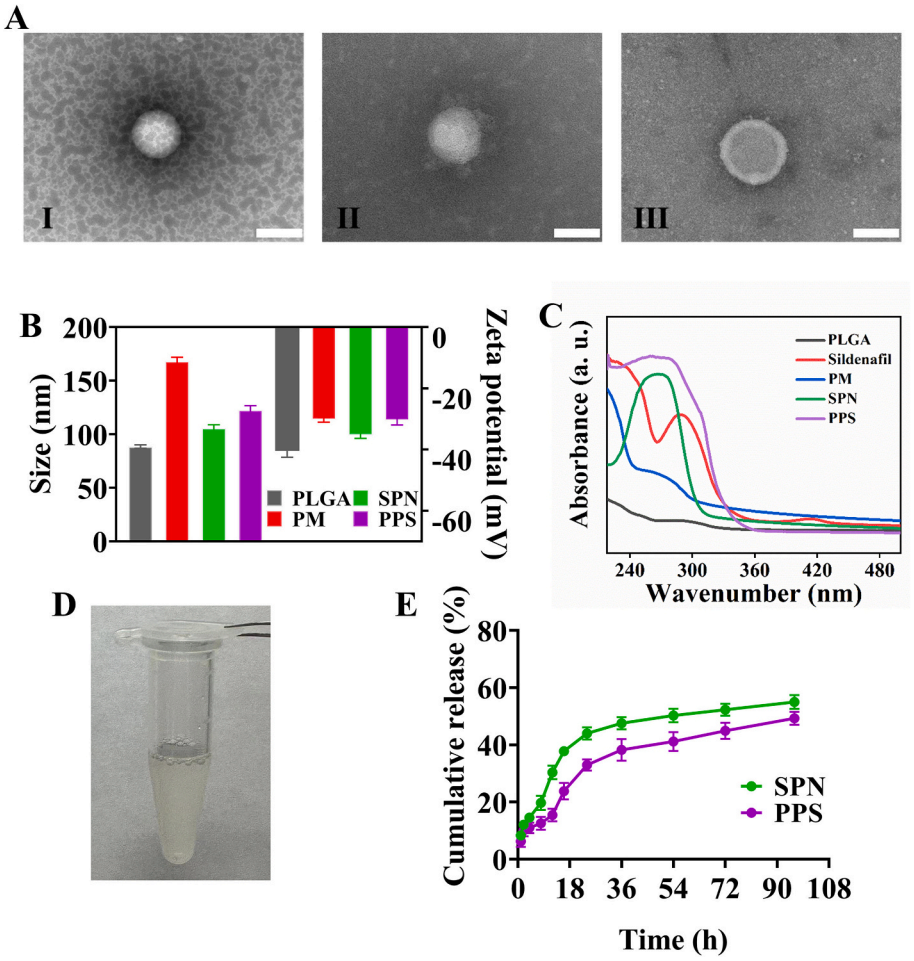

Fig. 2. Characterization of the nanoparticles. (A). TEM images of the PLGA (I), SPN (III) and PPS (III). Scale bar is 200 nm. (B). Particle size and zeta potential of different nanoparticles ($n = 3$). (C). UV–Vis absorbance of different nanoparticles. (D). Physical picture of aqueous solution of PPS. (E). In vitro release profiles of SPN and PPS in PBS at 37 °C ($n = 3$).

characterised by UV–Vis spectrophotometry (Fig. 2C), where sildenafil exhibited a typical absorption peak at 290 nm (Daraghmeh et al., 2001; Fejős et al., 2014). After loading sildenafil, PLGA showed a absorption peak between 260 and 280 nm. The PPS, integrating SPN and PM, displayed a broad absorption peak ranging from 240 to 300 nm, indirectly indicating the successful encapsulation of SNP by PM, which was consistent with previous experimental outcomes. The presence of key PM protein CD61 on the nanoparticles was confirmed via Western blot (Wu et al., 2020), demonstrating that PPS possessed an external protein environment very similar to PM (Fig. S1B). In addition, the hydrophobicity of PLGA was able to effectively encapsulate sildenafil into it. The loading efficiency of sildenafil in PLGA was 62.37% and the drug-loading was 16.51% as determined by high performance liquid chromatography (HLPC). The resulting PPS solution appeared as a slightly milky solution (Fig. 2D). Based on the drug-loading of the PPS, it was calculated that 6.06 mg of PPS contained 1 mg of sildenafil. For better quantitative analysis, the PPS containing 1 mg of sildenafil was designated as 1 unit.

To evaluate the drug release from PPS in vitro, the detection of free sildenafil using HLCP and the in vitro drug release curve of PPS at 37 °C was investigated (Fig. 2E) (Rescignano et al., 2016). In SNP, approximately 40% of the drug was released from PLGA within 16 h, while it took about 36 h for PPS to release 40% of the drug. The release rate of sildenafil from PLGA by PPS was slightly slower than SNP, but there was little difference in the efficiency of the final drug release between SNP and PPS. This demonstrated that nanoparticles encapsulated by PM could release the drug more slowly.

3.2. *In vitro cellular experiment and biosafety of PPS*

Good cytocompatibility is a prerequisite for PPS application. Therefore, to evaluate the cytocompatibility of PPS in vitro, HUVECs were co-cultured with sildenafil or PPS, respectively, and the cell viability was assessed by CCK-8 assay at 12 and 48 h. The cell viability of the HUVECs showed no significant difference compared to the control group (Fig. 3A). Additionally, live/dead staining of HUVECs was also performed at 48 h (Fig. S2) and the results were consistent with the results of CCK-8 assay, which indicated that PPS had good cellular compatibility.

The migratory capacity of HUVECs and VSMCs plays a crucial role in vascular healing and intimal hyperplasia (Ma et al., 2017). In the cell scratch experiment, we evaluated the effects of PPS on the migration of HUVECs and VSMCs at 12 and 48 h. Firstly, PPS had a promoting effect on the migration of HUVECs (Fig. S3A). Compared to the control group, PPS increased HUVECs migration rate by 24.22% and 20.11% at 12 and 48 h, respectively (Fig. 3B), suggesting that PPS supported the endothelial repair process by promoting cell migration. This result indicated that sildenafil might play a positive role in angiogenesis and endothelial repair. In contrast, PPS inhibited the migration of VSMCs (Fig. S3B). In the VSMCs cell scratch assay, migration rate of PPS-treated cells was

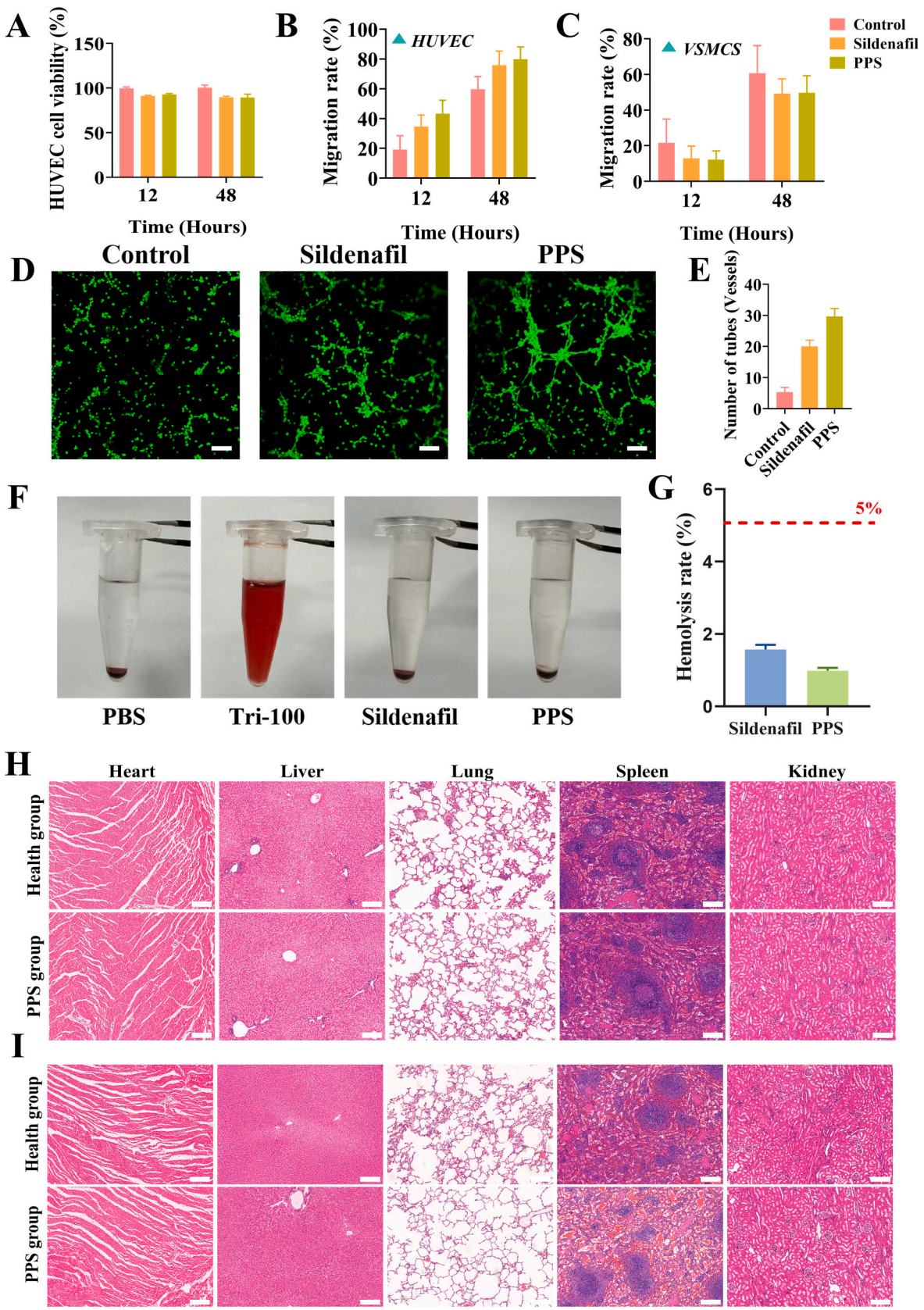

Fig. 3. In vitro cell assay and biosafety of PPS. (A). CCK-8 assay of cell viability after co-incubation of PPS or sildenafil with HUVECs ($n = 5$). (B). Cell migration rate of HUVECs co-incubated with PPS or Sildenafil ($n = 3$). (C). Cell migration rate of VSMCs co-incubated with PPS or Sildenafil ($n = 3$). (D). Tube formation assay of HUVECs co-incubated with PPS or Sildenafil. Scale bar is 100 μm. (E). Quantitative analysis of tube formation in the tube formation assay ($n = 3$). (F). Hemolysis assay of sildenafil and PPS. (G). The hemolysis rate corresponding to Fig. (F) ($n = 5$). (H) and (I) HE staining of major organs (kidneys, lungs, spleen, liver and heart). To evaluate the effect of PPS on the major organ functions of health and model rabbits. Scale bar is 200 μm.

slower, with a decrease of 16.23% and 18.97%, compared with that in the control group at 12 and 48 h, respectively. This suggested that PPS might reduce the risk of endothelial hyperplasia by inhibiting smooth muscle cell migration implying sildenafil might have a potential therapeutic role in preventing vascular diseases such as blood vessel stenosis and atherosclerosis. Overall, the cell scratch assay demonstrated that PPS effectively promoted the migration of HUVECs and significantly inhibited the migration of VSMCs.

The tube formation assay is important for studying vascular diseases and therapeutic strategies for vascular-related diseases (Pyriochou et al., 2007). The role of PPS in promoting angiogenesis and tissue repair was evaluated through a tube formation assay using HUVECs. Compared with the untreated control group, the sildenafil and PPS groups exhibited more tubular structures (Fig. 3D), which was clearly confirmed through quantitative analysis of tube formation (Fig. 3E). These experimental results indicated that the PPS possessed the capability to enhance the tube formation in HUVECs. Furthermore, this discovery revealed the potential of PPS in promoting vascular endothelial cell function. Intimal hyperplasia is a primary cause of late stenosis and occlusion formation in vein grafts, whereas the overgrowth of VSMCs is the main cause of intimal hyperplasia (Feng et al., 2022). At 48 h, the proliferation rate of the control group reached approximately 129.59%, while that of the PPS group was close to 95.94% (Fig. S4), indicating PPS could effectively inhibit the overproliferation of VSMCs (Tantini et al., 2005). These experimental results suggested that inhibiting the overproliferation of VSMCs possibly served as an important mechanism for PPS to inhibit intimal hyperplasia. To sum up, in vitro cellular experiments have confirmed the potential application value of PPS in treating vascular diseases.

To investigate the in vivo safety of PPS, a hemolysis test was performed with 1 mL of rabbit blood taken from the marginal ear vein, and the PPS was co-incubated with blood at 37 °C for 8 h (Fig. 3F). It can be seen that PPS did not cause obvious haemolysis compared with the negative control group and the haemolysis rate was much lower than the 5% critical value (Fig. 3G), demonstrating excellent haemocompatibility of PPS. Furthermore, we injected PPS into the mice through the marginal ear vein and then collected tissue samples from major organs including the heart, liver, spleen, lungs and kidneys at 1 and 28 days after injection to perform HE staining (Fig. 3H-I). Compared to the healthy group, no obvious pathological differences were observed in these organs after PPS treatment, indicating its prominent biocompatibility in vivo. In summary, these experimental results suggested that PPS offered a good safety profile for in vivo applications.

3.3. Evaluation of the targeting ability of PPS in vein graft model

Platelet membrane-coated nanoparticles could be recruited at the site of vascular endothelial injury. During the vein graft surgery, mechanical injury to the vascular endothelium was responsible for the exposure of subendothelial extracellular matrix (ECM), which in turn recruited platelets. Furthermore, platelets bound to the damaged vessels through multifactor receptor-ligand interactions (Wang et al., 2020). Therefore, the ability to target vein graft could be achieved by encapsulating PM on the surface of nanoparticles. The targeting ability of PPS was evaluated using a rabbit model of vein graft. Control and experimental group rabbits (after vein grafting) were administered PPS labelled with DiD dye intravenously via the marginal ear vein. Fluorescence signals were detected in the vein grafts, contralateral normal blood vessels along with in the major organs (heart, liver, spleen, lungs and kidneys) of the rabbits at different time points after injection (Fig. 4A). In the experimental group rabbits, significant fluorescence signals were observed on the vein graft, while there were no significant fluorescent signals in the contralateral normal vein and normal blood vessels in the healthy group, suggesting that PPS could target vein graft. This indicates that PPS can target vein graft. Meanwhile, obvious fluorescence signals were also observed in the liver, kidney and spleen of rabbits. Quantitative analysis of the fluorescence intensity (Fig. 4B-D) showed that the average fluorescence intensity was the strongest in the vein grafts, followed by the liver with the fluorescence intensity gradually diminishing over time. At 6 h, a distinct fluorescence signal appeared on the vein graft, with the intensity decreasing over time (Fig. 4E). At 12 h, the fluorescence intensity of the vein graft was decreased by approximately 39.89% (Fig. 4F). These results further confirmed that the platelet membrane-encapsulated nanoparticles exhibited certain targeting ability to the vein graft, making them ideally suited for targeted delivery of anti-intimal hyperplasia drugs to the desired site. However, the PPS also accumulated in some organs and drug concentrations decreased markedly within 24 h owing to metabolism in organs, such as the liver (Cai et al., 2020; Jin et al., 2024; Shen et al., 2020).

In addition, to understand the release of sildenafil in vivo, rabbits in the two experimental groups were administered with either sildenafil or PPS via the marginal ear vein and plasma sildenafil levels were measured by HLPC at different time points (Fig. 4G). After direct intravenous injection of sildenafil, plasma levels of sildenafil peaked rapidly and declined to low levels after 4 h. Compared to direct sildenafil injection, the plasma concentration of sildenafil peaked at about 8 h after PPS injection and the blood concentration of sildenafil could be maintained in the desired range within 48 h. These experimental results demonstrated that PPS could slowly release sildenafil in vivo and maintained effective blood concentrations for a long time. The slow release behaviour of PPS provided a certain level of nanoparticles at the vein graft site before drug released, and meanwhile reduced the risk of side effects caused by the premature and excessive release of sildenafil before the PPS reached the target location, as well as minimized the number of administrations as compared to direct intravenous injection of sildenafil.

3.4. Vascular ultrasound assesses the therapeutic efficacy of PPS

Subsequently, we studied the therapeutic effect of PPS on intimal hyperplasia of vein graft in vivo. New Zealand rabbits are medium-sized animals that are much easier to operate on than smaller animals, and more cost-effective than larger animals. Therefore, they are highly suitable for creating vein graft animal models (Anderson et al., 2018). In this study, a rabbit vein graft model was established using the “cuff” method to simulate clinical bypass surgery (Wong et al., 2008; Wu et al., 2018). The overall animal experimental procedure is shown in Fig. 5. All rabbits were divided into four groups: the blank group, the control group, the sildenafil group and the PPS group. The blank group served as a sham surgery group, where only the external jugular vein of the rabbits was freed without further procedure and the remaining three groups underwent vein grafting surgery (Fig. 6A). After the operation, the control, the sildenafil and the PPS groups were injected with saline, sildenafil, and PPS, respectively. Ultrasonography stands out for vascular assessment due to its non-invasive nature, real-time functionality, and exceptional accuracy (Fig. 6B) (Somarathna et al., 2022). Hence, ultrasound inspections of rabbits vessels was performed in each group at different time points (Fig. 6C). Throughout the entire experimental process, the vascular diameter remained unchanged in the blank group, indicating that the sham operation did not induce any vascular damage. In contrast to the blank group, the vascular diameter of the grafted vein showed a notable increase post-surgery in the other three groups. The increase in vascular diameter post-surgery in the transplanted veins is attributed to their adaptation and dilation to accommodate the higher pressure and flow rates associated with arterial location. In the control group, a significant narrowing of the grafted veins in rabbits was observed, likely due to the higher blood pressure and flow velocity in arteries, leading to endothelial damage caused by arterial impact, which is one of the contributing factors to intimal hyperplasia (Qiu et al., 2023). There was a significant improvement in the narrowing of the vascular diameter in the sildenafil or PPS groups on 14

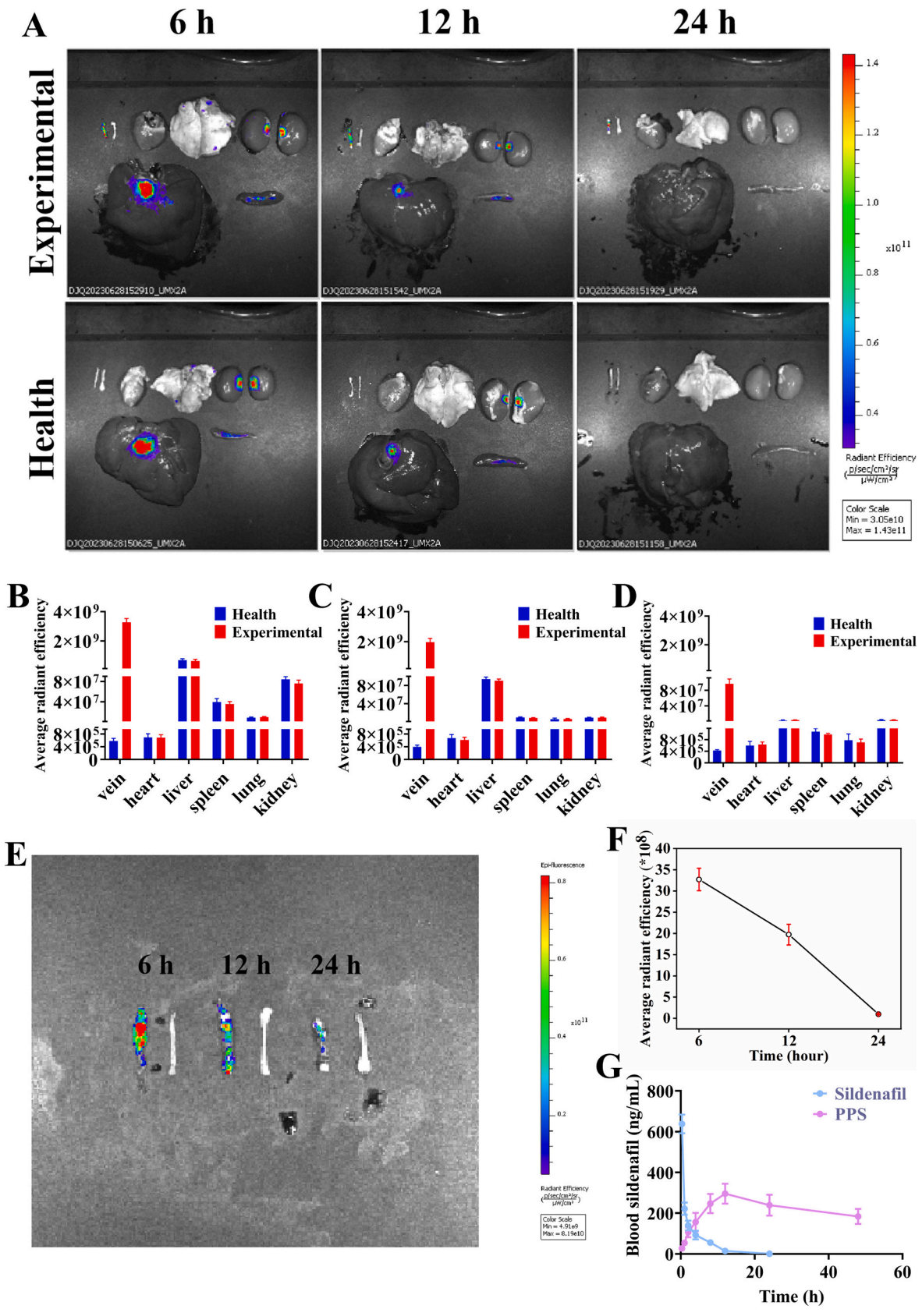

Fig. 4. Evaluation of PPS targeting capability. (A). Distribution of DiD-stained PPS in vein graft, normal blood vessels and major organs (heart, liver, spleen, lungs and kidneys). Quantitative analysis of the mean fluorescence intensity of the different organs in Fig. (A) was performed at 6 (B), 12 (C) and 24 (D) hours, respectively ($n = 3$). (E). Fluorescence images of isolated blood vessels (6, 12 and 24 h) from rabbits in the PPS group. (F). Quantitative analysis of the mean fluorescence intensity of isolated blood vessels ($n = 3$). (G). Plasma concentration-time curves after intravenous injection of sildenafil or PPS in rabbits of the experimental groups ($n = 3$).

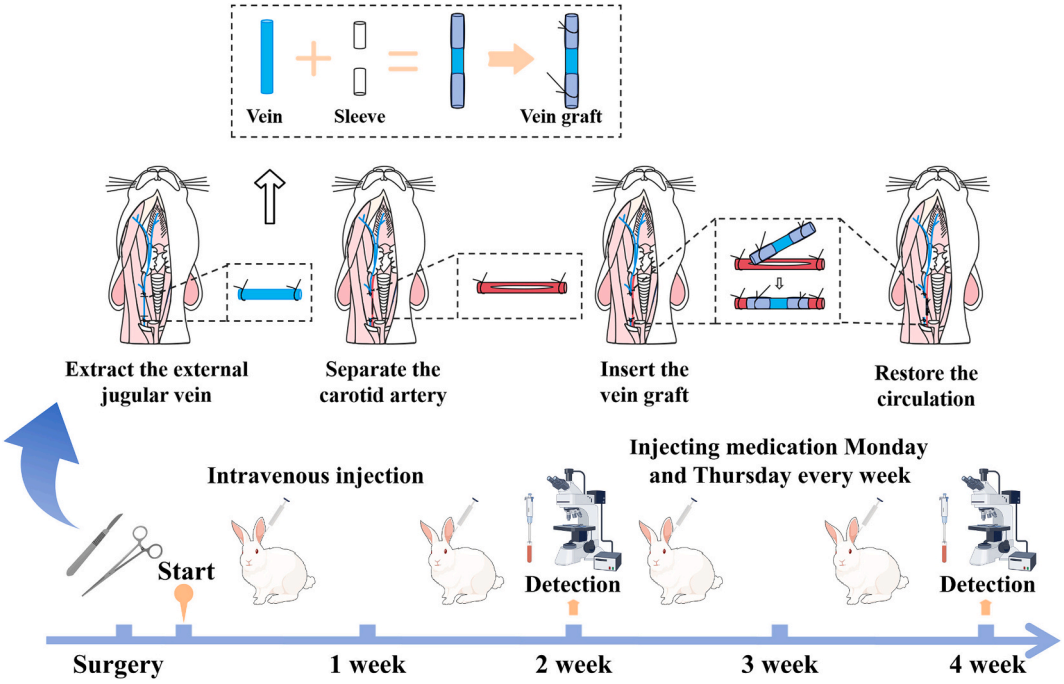

Fig. 5. Schematic illustration of a rabbit model of intimal hyperplasia of vein grafts by the "Cuff" method and the overall animal experimental procedure.

and 28 days compared to the control group. Simultaneously, quantitative analysis of vascular stenosis rate revealed no significant difference between the sildenafil and PPS groups on day 14, but by day 28, the stenosis rate in the PPS group was lower than that in the sildenafil group. This suggested that the inhibitory ability of PPS on vascular stenosis might be superior to that of direct sildenafil injection with prolonged treatment duration. Moreover, the flow velocity of blood vessels was detected by vascular ultrasound (Fig. S5, Fig. 6E). The reduced vascular flow velocity observed in both the sildenafil and PPS groups,compared to the control group, might be attributed to increased flow rates induced by vascular stenosis in the control group, while effective inhibition of vascular stenosis could result in a decrease in vascular flow velocity. This also indirectly indicated that PPS could effectively inhibit vascular stenosis caused by intimal hyperplasia.

3.5. *Histological evaluation the therapeutic efficacy of PPS*

The advantage of histological evaluation in assessing therapeutic efficacy lies in its ability to visually observe changes in tissue structure, thereby evaluating treatment outcomes. Next, we assessed the efficacy of PPS in inhibiting intimal hyperplasia in a rabbit model of vein graft intimal hyperplasia through histological staining. Firstly, we examined whether the PPS could inhibit intimal hyperplasia of grafted vein in vivo by HE staining (Fig. 7A). Compared to the control group, significant inhibition of intimal hyperplasia development was observed in both the sildenafil and PPS groups on 14 and 28 days (Fig. 7B). Quantitative analysis of the intimal thickness showed that at 28 day, the control group exhibited a thickness of 172.77 ± 6.50 μm, whereas the PPS group showed only 112.30 ± 8.02 μm. Importantly, the intimal thickness in the PPS group was lower than that in the sildenafil group (Fig. 7C), consistent with previous vascular ultrasound findings. The ratio of intima to media thickness serves as an indicator of the extent of intimal hyperplasia (Orban et al., 2021), with an elevated ratio commonly indicating vascular narrowing. By analysing the intima-to-media ratio in each group, at 28 day, the intima-media ratio in the control group was 2.28 ± 0.14, whereas in the sildenafil and the PPS groups, it was 1.83 ± 0.11, 1.39 ± 0.09, respectively (Fig. 7D), showing that the PPS group could effectively inhibit the extent of intimal hyperplasia with its efficacy surpassing that of the sildenafil group. Intimal hyperplasia often accompanies an increase in collagen fiber deposition and masson staining, which highlights blue collagen fibers, aids in assessing the severity of neointimal hyperplasia and its relationship with fibrosis (Pelliccia et al., 2021). Masson staining showed that the severity of intimal hyperplasia in the PPS group was significantly reduced compared to the control group (Fig. 7E). Quantitative analysis of masson staining, at 14 and 28 days, indicated that the collagen fiber content in the PPS group was lower than that in the control group. An increase in collagen deposition often leads to intimal thickening and reconstruction of the vessel wall, thus aggravating the abnormal changes in the vessel wall. The experimental findings demonstrated that the PPS could reduce collagen deposition in the vessel wall and inhibit intimal hyperplasia. In conclusion, PPS exhibits notable efficacy in inhibiting intimal hyperplasia in vivo.

3.6. *Therapeutic effects of PPS*

Intimal hyperplasia is closely associated with excessive proliferation of smooth muscle cells, deposition of ECM and a persistent inflammatory process (Maruf et al., 2019; Wang et al., 2019; Yang et al., 2022). Within the pathological milieu of intimal hyperplasia, elevated levels of CD68 reflect active inflammation responses and cellular immune involvement, typically positively correlated with the extent of intimal hyperplasia, thus serving as a measurable indicator of disease severity and inflammation-related pathological changes (Glass et al., 2019). Immunohistochemical (IHC) staining of vascular tissues revealed the control group exhibited increased CD68 expression in the vein graft, while the PPS group showed decreased CD68 expression, compared to the blank group (Fig. 8A). Alpha-smooth muscle actin (α-SMA) is a pivotal marker protein for smooth muscle cells (SMCs), playing a crucial role in neointimal hyperplasia. When the vascular intima is damaged or subjected to pathological stimuli, SMCs transition from a contractile phenotype to a synthetic phenotype, leading to increased expression of α-SMA and subsequent intimal hyperplasia (Xie et al., 2018). IHC staining for α-SMA indicated that the PPS group effectively reduced the expression of α-SMA, compared to the control group (Fig. 8B). Vascular re-endothelialization plays a critical role in preventing neointimal

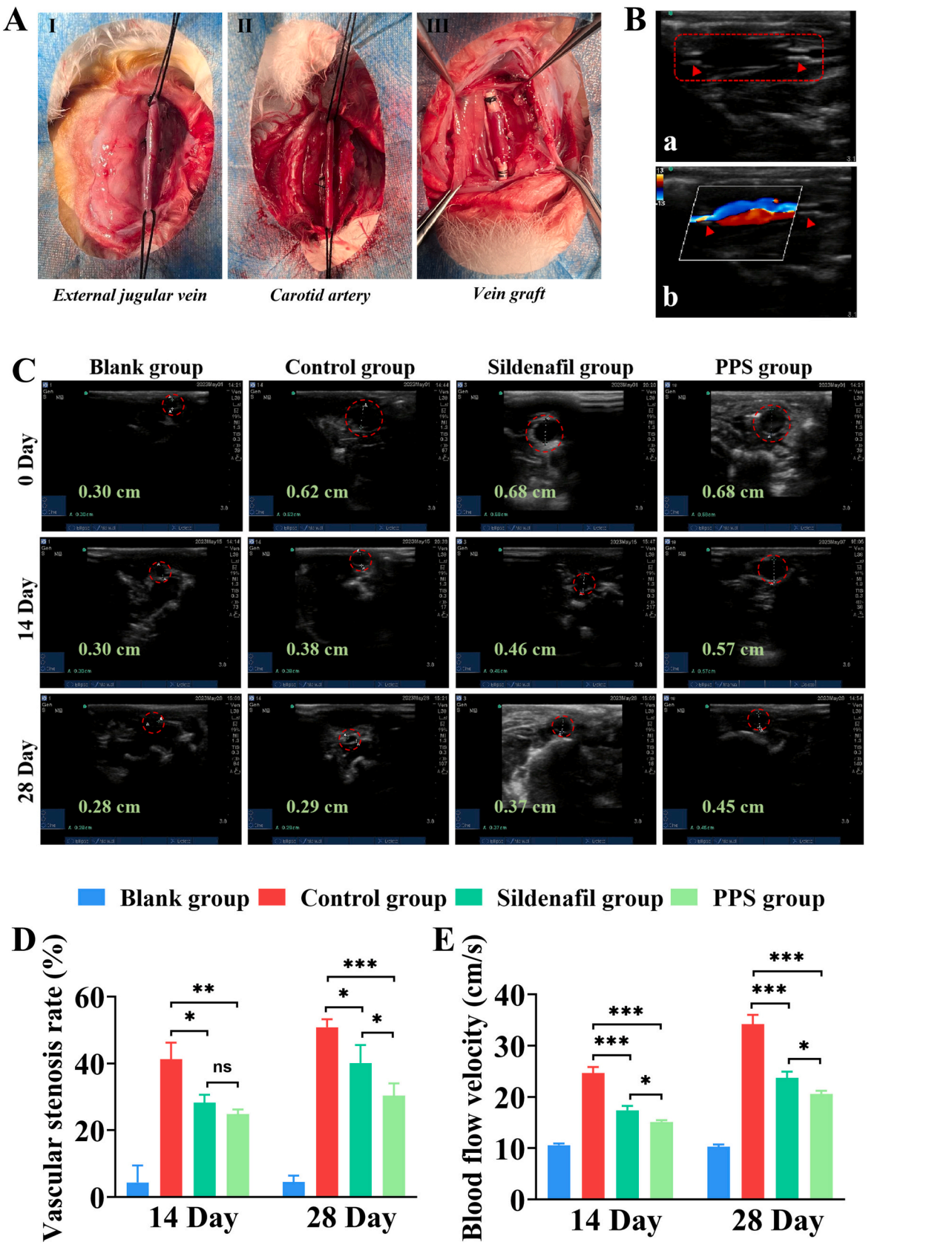

Fig. 6. Vascular ultrasound assessment of therapeutic efficacy. (A). Schematic diagram of molding using "Cuff" method. (B). Vascular ultrasound of the vein graft. (C). Vascular ultrasound evaluation of the diameter changes in the vein graft of each group of rabbits at 14 and 28 days. (D). Stenosis rate of vein graft in each group of rabbits at 14 and 28 days ($n = 3$). (E). Blood flow velocity of vein graft in each group of rabbits at 14 and 28 days ($n = 3$). All data are shown as the mean ± SD. Compared with Control group, $^{*}p < 0.05$, $^{**}p < 0.01$, $^{***}p < 0.001$.

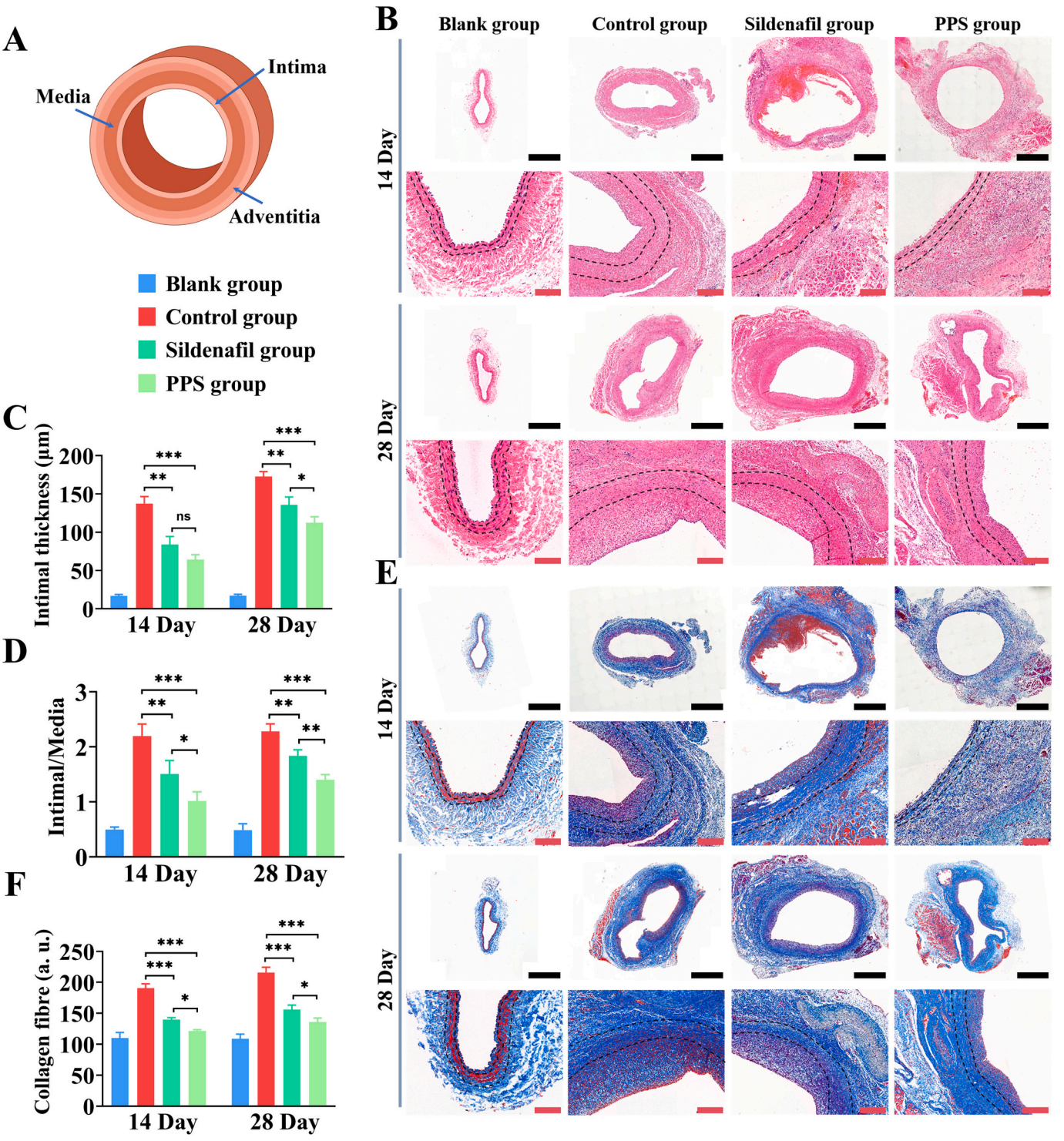

Fig. 7. Histological staining evaluation of therapeutic efficacy. (A). Diagram of Blood Vessel Layers. (B). HE staining of vein graft in rabbits at 14 and 28 days. Black scale 1 mm, red scale 200 μm. (C). Intimal thickness of vein graft in rabbits at 14 and 28 days ($n = 3$). (D). The ratio of intima to media of vein graft in rabbits at 14 and 28 days ($n = 3$). (E). Masson staining of vein graft in rabbits at 14 and 28 days. Black scale is 1 mm, red scale is 200 μm. (F). Quantitative analysis of collagen fibers stained with Masson in vein graft of rabbits at 14 and 28 days ($n = 3$). All data are shown as the mean ± SD. Compared with Control group, $^{*}p < 0.05$, $^{**}p < 0.01$, $^{***}p < 0.001$. (For interpretation of the references to color in this figure legend, the reader is referred to the web version of this article.)

hyperplasia, including maintaining the integrity of the endothelium, suppressing inflammatory responses, sustaining vascular barrier function, and regulating vascular tone. CD31 is an important indicator for assessing the re-endothelialization processes (Bruggisser et al., 2020; Zhao et al., 2023). Therefore, anti-CD 31 antibody was used for IHC staining of blood vessels to assess the process of re-endothelialisation. In comparison with the normal vascular tissues in the blank group, the control group showed lower expression of CD31, indicative of reduced endothelialization, whereas both the sildenafil and PPS groups exhibited increased CD31, signifying significantly enhanced endothelialization (Fig. 8C). Subsequently, quantitative analysis of all IHC staining results revealed (Fig. 8D-F) that compared to the control group, the PPS group

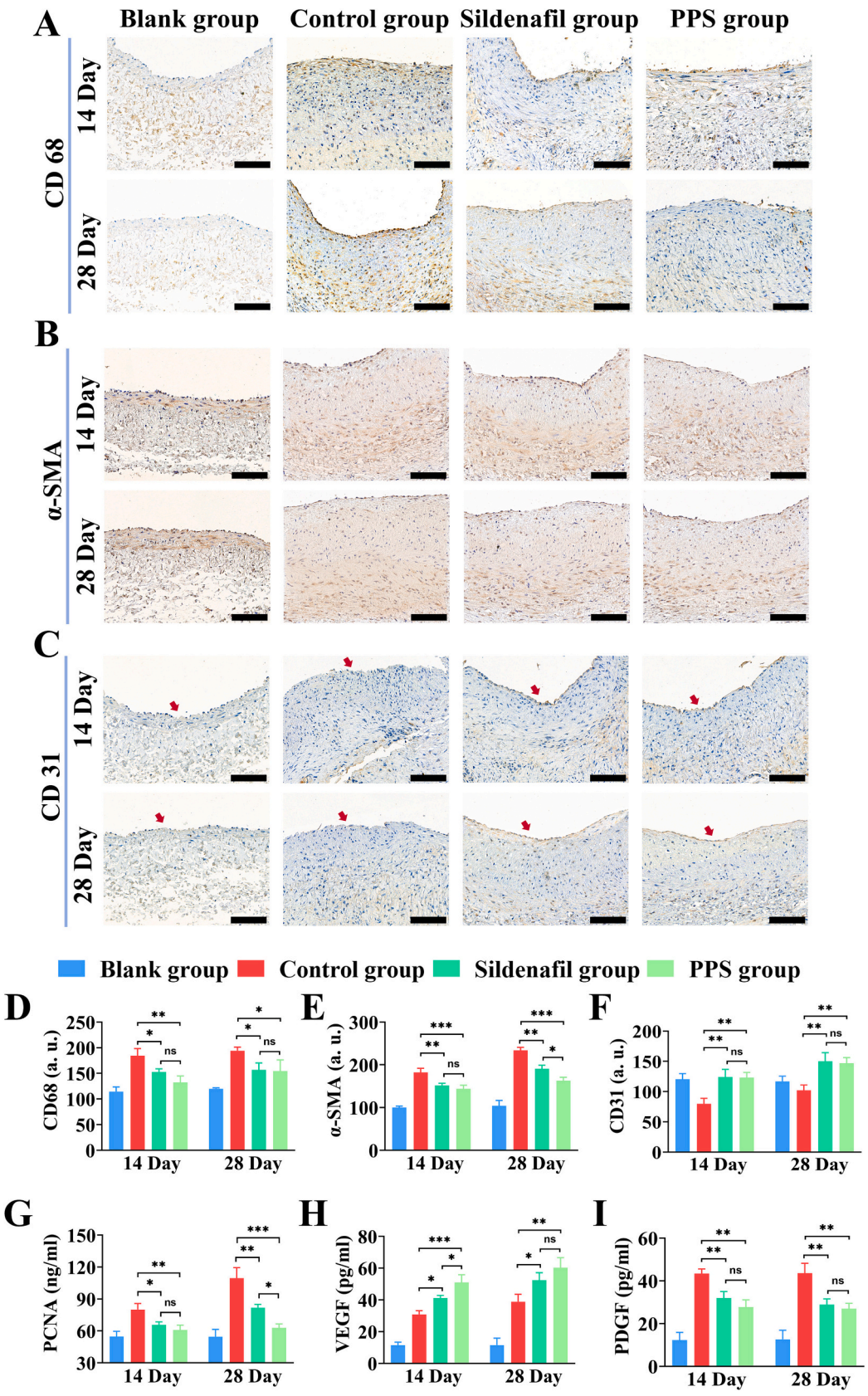

Fig. 8. Analysis of the therapeutic effects of PPS. Immunohistochemical staining of CD68 (A), α-SMA (B) and CD31 (C) in vein graft of rabbits at 14 days and 28 for each group. Quantitative analysis of the expression levels of CD68 (D), α-SMA (E) and CD31 (F) in vein graft of rabbits for each group ($n = 3$). scale is 100 μm. ELISA analysis of the changes in the content of PCNA (G), VEGF (H) and PDGF (I) in vein graft tissues of rabbits for each group at 14 and 28 days ($n = 3$). All data are shown as the mean ± SD. Compared with Control group, $^{*}p < 0.05$, $^{**}p < 0.01$, $^{***}p < 0.001$.

demonstrated a decrease in CD68 and α-SMA expression intensities by 28.32% (14 day), 20.54% (28 day), and 21.09% (14 day), 36.32% (28 day), respectively, while CD31 expression intensity increased by 35.22% (14 day), 30.31% (28 day). These findings indicated that the PPS could effectively inhibit inflammatory responses and excessive proliferation of vascular smooth muscle cells in vein graft in vivo, promote endothelial maturation and restore endothelial function, thereby inhibiting intimal hyperplasia.

In addition, to further evaluate the therapeutic effect of PPS on vein graft. The contents of PCNA, VEGF, PDGF, TNF-α and IL-1β in the vein grafts tissues were measured using appropriate enzyme-linked immunosorbent assay (ELISA). PCNA, a marker of cell proliferation, exhibits significantly increased expression during active proliferation of VSMCs (Juan and Qian-Hui, 2018). At 14 and 28 days, compared to the control group, both the sildenafil and PPS groups exhibited significantly reduced PCNA levels in grafted vein tissues (Fig. 8G), with the PPS group showing lower PCNA levels than the sildenafil group at 28 day, suggesting that PPS acted to inhibit intimal hyperplasia by reducing VSMCs proliferation and suppressing PCNA expression. VEGF, the main driver of angiogenesis, exerts a vital influence on the vascular regeneration, particularly in endothelial repair and re-endothelialization after vascular injury (Liu et al., 2022). Compared to the control group, VEGF content increased in vein graft tissues after treatment with sildenafil or PPS, with the PPS group showing a 28-day increase of 21.51 ± 1.78 pg/mL, akin to that of the sildenafil group (Fig. 8H). This result substantiated this demonstration that PPS potentially increased the expression of VEGF and promote the endothelial cell proliferation and migration to the damaged area, which contributed to vascular repair and re-endothelialisation post-injury, thus restoring normal vascular function and preventing further development of intimal hyperplasia. Blocking or modulating PDGF and its receptor is considered as a potential strategy for the treatment of intimal hyperplasia (Hwang et al., 2023). By examining PDGF level in the grafted vein tissues, PPS decreased PDGF levels at 14 and 28 days compared to the control group, with reductions of 15.74 ± 4.29 pg/mL and 16.58 ± 7.04 pg/mL respectively (Fig. 8I). This indicated that PPS could inhibit the expression of PDGF, thereby suppressing intimal hyperplasia and slowing down vascular narrowing process. Endothelial injury typically triggers an inflammatory response, wherein excessive or persistent inflammation leads to intimal hyperplasia and restenosis. TNF-α and IL-1β are key inflammatory markers within the inflammatory responses (Fig. S6A—B). At 14 day post-vein grafting, the content of TNF-α and IL-1β in the vein grafts tissues of the control group reached 86.07 ± 6.38 pg/mL and 73.11 ± 7.14 pg/mL, respectively, but by 28 day, these levels decreased, likely related to the natural decline of inflammatory factors as a result of the individual immune responses. In the vein graft tissues of rabbits treated with sildenafil or PPS, compared to the control group, the contents of TNF-α and IL-1β were significantly reduced, with reductions of 30.81 ± 9.05 pg/mL and 17.13 ± 8.71 pg/mL, respectively, by 28 day. This indicated that PPS possessed a significant effect in inhibiting the inflammatory response in the vein graft.

In summary, PPS exhibits significant capabilities in inhibiting intimal hyperplasia and inflammation, maintaining vascular patency, and avoiding stenosis and occlusion of vein grafts. Moreover, compared to using sildenafil alone, the therapeutic advantages of PPS on vein grafts become increasingly evident with prolonged treatment duration.

4. Conclusion

After vein transplantation, intimal hyperplasia emerges as a significant factor in vein grafts restenosis. In this study, we devised the platelet membrane-coated PLGA nanoparticles loaded with sildenafil (PPS) for precision treatment of post-transplant intimal hyperplasia. In vitro cellular experiments validated the therapeutic potential of PPS in inhibiting intimal hyperplasia. Furthermore, within an animal model of intimal hyperplasia in vein graft, PPS demonstrated outstanding targeting precision, facilitating gradual sildenafil release, fostering vascular endothelialization, curbing the migration and proliferation of smooth muscle cells and modulating the inflammatory responses, thus countering intimal hyperplasia. Notably, PPS exhibited favourable biocompatibility. In conclusion, this biomimetic nanocarrier holds tremendous promise in the treatment of intimal hyperplasia.

Funding statement

This work was supported by a grant from the Science and Technology Bureau of Wenzhou City, Zhejiang Province, China (Y2020046).

Ethics approval statement

In this study, we strictly adhered to the ARRIVE guidelines (Animal Research: Reporting of In Vivo Experiments). All experimental animals was approved by the Ethics Committee of Wenzhou Medical University (Approval number.: wydw2023–0233), and we described the process of animal experiments in accordance with the guidelines. We are committed to maintaining animal welfare and minimizing the negative impact of experimental procedures on animals.

Permission to reproduce material from other sources

No.

CRediT authorship contribution statement

Fajing Yang: Writing – original draft, Methodology, Investigation. **Yihui Qiu:** Validation, Formal analysis, Data curation. **Xueting Xie:** Validation, Formal analysis. **Xingjian Zhou:** Formal analysis. **Shunfu Wang:** Formal analysis. **Jialu Weng:** Formal analysis. **Lina Wu:** Formal analysis. **Yizhe Ma:** Formal analysis. **Ziyue Wang:** Formal analysis. **Wenzhang Jin:** Supervision, Methodology, Investigation, Conceptualization. **Bicheng Chen:** Resources, Funding acquisition, Conceptualization.

Declaration of competing interest

The authors declare no potential conflicts of interest with respect to the research, authorship, and publication of this article.

Data availability of statement

Data available on request from the authors.

Acknowledgments

This work was supported by a grant from the Science and Technology Bureau of Wenzhou City, Zhejiang Province, China (Y2020046). The staff of the Experimental Animal Center of Wenzhou Medical University provided valuable assistance in the successful completion of the experiments.

Appendix A. Supplementary data

Supplementary data to this article can be found online at https://doi.org/10.1016/j.ijpx.2024.100278.

References

Al-Hroub, H., Alkhawaja, B., Alkhawaja, E., Arafat, T., 2016. Sensitive and rapid HPLC-UV method with back-extraction step for the determination of sildenafil in human plasma. J. Chromatogr. B 1009, 1–6.

Anderson, D.E., Pohan, G., Raman, J., Konecny, F., Yim, E.K., Hinds, M.T., 2018. Improving surgical methods for studying vascular grafts in animal models. Tissue Eng. Part C: Meth. 24, 457–464.

Beerkens, F.J., Claessen, B.E., Mahan, M., Gaudino, M.F., Tam, D.Y., Henriques, J.P., Mehran, R., Dangas, G.D., 2022. Contemporary coronary artery bypass graft surgery and subsequent percutaneous revascularization. Nat. Rev. Cardiol. 19, 195–208.
Bongaarts, A., van Scheppingen, J., Korotkov, A., Mijnsbergen, C., Anink, J.J., Jansen, F. E., Spliet, W.G., den Dunnen, W.F., Gruber, V.E., Scholl, T., 2020. The coding and non-coding transcriptional landscape of subependymal giant cell astrocytomas. Brain 143, 131–149.
Bruggisser, J., Tarek, B., Wyder, M., Müller, P., von Ballmoos, C., Witz, G., Enzmann, G., Deutsch, U., Engelhardt, B., Posthaus, H., 2020. CD31 (PECAM-1) serves as the endothelial cell-specific receptor of Clostridium perfringens β-toxin. Cell Host Microbe 28, 69–78 (e66).
Cai, Y., Xu, Z., Shuai, Q., Zhu, F., Xu, J., Gao, X., Sun, X., 2020. Tumor-targeting peptide functionalized PEG-PLA micelles for efficient drug delivery. Biomater. Sci. 8, 2274–2282.
Charakida, M., Tousoulis, D., 2013. Biomarkers of Peripheral Arterial Disease. Biomark. Cardiovasc. Diseases 210.
Cole, J.W., 2017. Large artery atherosclerotic occlusive disease. CONTINUUM. Lifelong Learn. Neurol. 23, 133–157.
Dahshan, H.E., Helal, M.A., Mostafa, S.M., Elgawish, M.S., 2019. Development and validation of an HPLC-UV method for simultaneous determination of sildenafil and tramadol in biological fluids: Application to drug-drug interaction study. J. Pharm. Biomed. Anal. 168, 201–208.
Daraghmeh, N., Al-Omari, M., Badwan, A., Jaber, A., 2001. Determinaton of sildenafil citrate and related substances in the commercial products and tablet dosage form using HPLC. J. Pharm. Biomed. Anal. 25, 483–492.
Dashwood, M.R., Loesch, A., 2007. Surgical damage of the saphenous vein and graft patency. J. Thorac. Cardiovasc. Surg. 133, 274–275.
Degjoni, A., Campolo, F., Stefanini, L., Venneri, M.A., 2022. The NO/cGMP/PKG pathway in platelets: The therapeutic potential of PDE5 inhibitors in platelet disorders. J. Thromb. Haemost. 20, 2465–2474.
Fejős, I., Neumajer, G., Béni, S., Jankovics, P., 2014. Qualitative and quantitative analysis of PDE-5 inhibitors in counterfeit medicines and dietary supplements by HPLC–UV using sildenafil as a sole reference. J. Pharm. Biomed. Anal. 98, 327–333.
Feng, L.-A., Shi, J., Guo, J.-Y., Wang, S.-F., 2022. Recent strategies for improving hemocompatibility and endothelialization of cardiovascular devices and inhibition of intimal hyperplasia. J. Mater. Chem. B 10, 3781–3792.
Glass, C., Butt, Y.M., Gokaslan, S.T., Torrealba, J.R., 2019. CD68/CD31 immunohistochemistry double stain demonstrates increased accuracy in diagnosing pathologic antibody-mediated rejection in cardiac transplant patients. Am. J. Transplant. 19, 3149–3154.
Guazzi, M., 2008. Clinical use of phosphodiesterase-5 inhibitors in chronic heart failure. Circulation. Heart Failur. 1, 272–280.
Hamzehnejadi, M., Ranjbar Tavakoli, M., Abiri, A., Ghasempour, A., Langarizadeh, M.A., Forootanfar, H., 2022. A review on phosphodiesterase-5 inhibitors as a topical therapy for erectile dysfunction. Sex. Med. Rev. 10, 376–391.
Holinstat, M., 2017. Normal platelet function. Cancer Metastasis Rev. 36, 195–198.
Hu, C.-M.J., Fang, R.H., Wang, K.-C., Luk, B.T., Thamphiwatana, S., Dehaini, D., Nguyen, P., Angsantikul, P., Wen, C.H., Kroll, A.V., 2015. Nanoparticle biointerfacing by platelet membrane cloaking. Nature 526, 118–121.
Hwang, A.-R., Lee, H.-J., Kim, S., Park, S.-H., Woo, C.-H., 2023. Inhibition of p90RSK ameliorates PDGF-BB-mediated phenotypic change of vascular smooth muscle cell and subsequent hyperplasia of neointima. Int. J. Mol. Sci. 24, 8094.
Jin, W., Xie, X., Shen, S., Zhou, X., Wang, S., Zhang, L., Su, X., 2024. Ultrasmall polyvinylpyrrolidone-modified iridium nanoparticles with antioxidant and anti-inflammatory activity for acute pancreatitis alleviation. J. Biomed. Mater. Res. A 112, 988–1003.
Juan, L., Qian-Hui, S., 2018. A6702 Dose-and time-effect relationship and mechanisms of proliferation of rat vascular smooth muscle cells stimulated by high sodium. J. Hypertens. 36, e18–e19.
Jung, S.-Y., Seo, Y.-G., Kim, G.K., Woo, J.S., Yong, C.S., Choi, H.-G., 2011. Comparison of the solubility and pharmacokinetics of sildenafil salts. Arch. Pharm. Res. 34, 451–454.
Kulkarni, S., Dopheide, S.M., Yap, C.L., Ravanat, C., Freund, M., Mangin, P., Heel, K.A., Street, A., Harper, I.S., Lanza, F., 2000. A revised model of platelet aggregation. J. Clin. Invest. 105, 783–791.
Ladak, S.S., McQueen, L.W., Layton, G.R., Aujla, H., Adebayo, A., Zakkar, M., 2022. The Role of Endothelial Cells in the Onset, Development and Modulation of Vein Graft Disease. Cells 11, 3066.
Lan, T.-H., Chen, X.-L., Wu, Y.-S., Qiu, H.-L., Li, J.-Z., Ruan, X.-M., Xu, D.-P., Lin, D.-Q., 2018. 3, 7-Bis (2-hydroxyethyl) icaritin, a potent inhibitor of phosphodiesterase-5, prevents monocrotaline-induced pulmonary arterial hypertension via NO/cGMP activation in rats. Eur. J. Pharmacol. 829, 102–111.
Lazo, R.E.L., de Paula Oliveira, B., de Fátima Cobre, A., Ferreira, L.M., Felipe, K.B., de Oliveira, P.R., Murakami, F.S., 2023. Engineering porous PLGA microparticles for pulmonary delivery of sildenafil citrate. Powder Technol. 430, 118999.
Liang, D., Walker, J., Schwendeman, P.S., Chandrashekar, A., Ackermann, R., Olsen, K. F., Beck-Broichsitter, M., Schwendeman, S.P., 2024. Effect of PLGA raw materials on in vitro and in vivo performance of drug-loaded microspheres. Drug Deliv. Translat. Res. 1–18.
Liu, X., Li, Y., Sun, Y., Chen, B., Du, W., Li, Y., Gu, N., 2022. Construction of functional magnetic scaffold with temperature control switch for long-distance vascular injury. Biomaterials 290, 121862.
Lordan, R., Tsoupras, A., Zabetakis, I., 2021. Platelet activation and prothrombotic mediators at the nexus of inflammation and atherosclerosis: Potential role of antiplatelet agents. Blood Rev. 45, 100694.
Ma, X., Jiang, C., Li, Y., Feng, L., Liu, J., Wang, J., 2017. Inhibition effect of tacrolimus and platelet-derived growth factor-BB on restenosis after vascular intimal injury. Biomed. Pharmacother. 93, 180–189.
Maruf, A., Wang, Y., Yin, T., Huang, J., Wang, N., Durkan, C., Tan, Y., Wu, W., Wang, G., 2019. Atherosclerosis Treatment with Stimuli-Responsive Nanoagents: recent advances and future perspectives. Adv. Healthc. Mater. 8, 1900036.
Mo, E., Amin, H., Bianco, I.H., Garthwaite, J., 2004. Kinetics of a cellular nitric oxide/cGMP/phosphodiesterase-5 pathway. J. Biol. Chem. 279, 26149–26158.
Mohebali, A., Abdouss, M., 2020. Layered biocompatible pH-responsive antibacterial composite film based on HNT/PLGA/chitosan for controlled release of minocycline as burn wound dressing. Int. J. Biol. Macromol. 164, 4193–4204.
Neufang, A., Espinola-Klein, C., Savvidis, S., Schmiedt, W., Poplawski, A., Vahl, C.F., Dorweiler, B., 2018. External polytetrafluoroethylene reinforcement of varicose autologous vein grafts in peripheral bypass surgery produces durable bypass function. J. Vasc. Surg. 67, 1778–1787.
Nilsson, D., Chess-Williams, R., Sellers, D., 2023. Phosphodiesterase-5 inhibitors tadalafil and sildenafil potentiate nitrergic-nerve mediated relaxations in the bladder vasculature. Eur. J. Pharmacol. 960, 176152.
Orban, M., Ulrich, S., Dischl, D., von Samson-Himmelstjerna, P., Schramm, R., Tippmann, K., Hein-Rothweiler, R., Strüven, A., Lehner, A., Braun, D., 2021. Cardiac allograft vasculopathy: differences of absolute and relative intimal hyperplasia in children versus adults in optical coherence tomography. Int. J. Cardiol. 328, 227–234.
Pelliccia, F., Gersh, B.J., Camici, P.G., 2021. Gaps in evidence for risk stratification for sudden cardiac death in hypertrophic cardiomyopathy. Circulation 143, 101–103.
Pyriochou, A., Zhou, Z., Koika, V., Petrou, C., Cordopatis, P., Sessa, W.C., Papapetropoulos, A., 2007. The phosphodiesterase 5 inhibitor sildenafil stimulates angiogenesis through a protein kinase G/MAPK pathway. J. Cell. Physiol. 211, 197–204.
Qi, W., Li, Q., Liew, C.W., Rask-Madsen, C., Lockhart, S.M., Rasmussen, L.M., Xia, Y., Wang, X., Khamaisi, M., Croce, K., 2017. SHP-1 activation inhibits vascular smooth muscle cell proliferation and intimal hyperplasia in a rodent model of insulin resistance and diabetes. Diabetologia 60, 585–596.
Qiu, Y., Xu, S., Chen, X., Wu, X., Zhou, Z., Zhang, J., Tu, Q., Dong, B., Liu, Z., He, J., 2023. NAD+ exhaustion by CD38 upregulation contributes to blood pressure elevation and vascular damage in hypertension. Signal Transduct. Target. Therapy 8, 353.
Rashid, J., Patel, B., Nozik-Grayck, E., McMurtry, I.F., Stenmark, K.R., Ahsan, F., 2017. Inhaled sildenafil as an alternative to oral sildenafil in the treatment of pulmonary arterial hypertension (PAH). J. Control. Release 250, 96–106.
Reffelmann, T., Kloner, R.A., 2003. Therapeutic potential of phosphodiesterase 5 inhibition for cardiovascular disease. Circulation 108, 239–244.
Rescignano, N., Tarpani, L., Romani, A., Bicchi, I., Mattioli, S., Emiliani, C., Torre, L., Kenny, J.M., Martino, S., Latterini, L., 2016. In-vitro degradation of PLGA nanoparticles in aqueous medium and in stem cell cultures by monitoring the cargo fluorescence spectrum. Polym. Degrad. Stab. 134, 296–304.
Restani, R.B., Pires, R.F., Baptista, P.V., Fernandes, A.R., Casimiro, T., Bonifácio, V.D., Aguiar-Ricardo, A., 2020. Nano-in-Micro sildenafil dry powder formulations for the treatment of pulmonary arterial hypertension disorders: the synergic effect of POxylated polyurea dendrimers, PLGA, and cholesterol. Part. Part. Syst. Charact. 37, 1900447.
Royse, A., Ren, J., Royse, C., Tian, D.H., Fremes, S., Gaudino, M., Benedetto, U., Woo, Y. J., Goldstone, A.B., Davierwala, P., 2022. Coronary artery bypass surgery without saphenous vein grafting: JACC review topic of the week. J. Am. Coll. Cardiol. 80, 1833–1843.
Salama, A.H., Mahmoud, A.A., Kamel, R., 2016. A novel method for preparing surface-modified fluocinolone acetonide loaded PLGA nanoparticles for ocular use: in vitro and in vivo evaluations. AAPS PharmSciTech 17, 1159–1172.
Shahin, H., Vinjamuri, B.P., Mahmoud, A.A., Mansour, S.M., Chougule, M.B., Chablani, L., 2021. Formulation and optimization of sildenafil citrate-loaded PLGA large porous microparticles using spray freeze-drying technique: a factorial design and in-vivo pharmacokinetic study. Int. J. Pharm. 597, 120320.
Shen, M.-Y., Chang, S.-H., Liu, T.-I., Lu, T.-Y., Sabu, A., Chen, H.-H., Chiu, H.-C., 2020. Combo-targeted nanoassemblies as a chemotherapy delivery system against peritoneal carcinomatosis colorectal cancer. Biomater. Sci. 8, 3885–3895.
Shishehbor, M.H., Jaff, M.R., 2016. Percutaneous therapies for peripheral artery disease. Circulation 134, 2008–2027.
Somarathna, M., Hwang, P.T., Millican, R.C., Alexander, G.C., Isayeva-Waldrop, T., Sherwood, J.A., Brott, B.C., Falzon, I., Northrup, H., Shiu, Y.-T., 2022. Nitric oxide releasing nanomatrix gel treatment inhibits venous intimal hyperplasia and improves vascular remodeling in a rodent arteriovenous fistula. Biomaterials 280, 121254.
Stipa, P., Marano, S., Galeazzi, R., Minnelli, C., Mobbili, G., Laudadio, E., 2021. Prediction of drug-carrier interactions of PLA and PLGA drug-loaded nanoparticles by molecular dynamics simulations. Eur. Polym. J. 147, 110292.
Tang, Y., Jia, Y., Fan, L., Liu, H., Zhou, Y., Wang, M., Liu, Y., Zhu, J., Pang, W., Zhou, J., 2022. MFN2 prevents neointimal hyperplasia in vein grafts via destabilizing PFK1. Circ. Res. 130, e26–e43.
Tantini, B., Manes, A., Fiumana, E., Pignatti, C., Guarnieri, C., Zannoli, R., Md, A.B., Galié, N., 2005. Antiproliferative effect of sildenafil on human pulmonary artery smooth muscle cells. Basic Res. Cardiol. 100, 131–138.
Vizza, C.D., Sastry, B., Safdar, Z., Harnisch, L., Gao, X., Zhang, M., Lamba, M., Jing, Z.-C., 2017. Efficacy of 1, 5, and 20 mg oral sildenafil in the treatment of adults with pulmonary arterial hypertension: a randomized, double-blind study with open-label extension. BMC Pulmon. Med. 17, 1–12.

Wang, S., Duan, Y., Zhang, Q., Komarla, A., Gong, H., Gao, W., Zhang, L., 2020. Drug targeting via platelet membrane–coated nanoparticles. Small Struct. 1, 2000018.
Wang, Y., Zhang, K., Qin, X., Li, T., Qiu, J., Yin, T., Huang, J., McGinty, S., Pontrelli, G., Ren, J., 2019. Biomimetic nanotherapies: red blood cell based core–shell structured nanocomplexes for atherosclerosis management. Adv. Sci. 6, 1900172.
Ward, A.O., Caputo, M., Angelini, G.D., George, S.J., Zakkar, M., 2017. Activation and inflammation of the venous endothelium in vein graft disease. Atherosclerosis 265, 266–274.
Wei, X., Ying, M., Dehaini, D., Su, Y., Kroll, A.V., Zhou, J., Gao, W., Fang, R.H., Chien, S., Zhang, L., 2018. Nanoparticle functionalization with platelet membrane enables multifactored biological targeting and detection of atherosclerosis. ACS Nano 12, 109–116.
Wong, A.P., Nili, N., Jackson, Z.S., Qiang, B., Leong-Poi, H., Jaffe, R., Raanani, E., Connelly, P.W., Sparkes, J.D., Strauss, B.H., 2008. Expansive remodeling in venous bypass grafts: novel implications for vein graft disease. Atherosclerosis 196, 580–589.
Wu, B., Werlin, E.C., Chen, M., Mottola, G., Chatterjee, A., Lance, K.D., Bernards, D.A., Sansbury, B.E., Spite, M., Desai, T.A., 2018. Perivascular delivery of resolvin D1 inhibits neointimal hyperplasia in a rabbit vein graft model. J. Vasc. Surg. 68, 188S–200S e184.
Wu, L., Xie, W., Zan, H.-M., Liu, Z., Wang, G., Wang, Y., Liu, W., Dong, W., 2020. Platelet membrane-coated nanoparticles for targeted drug delivery and local chemo-photothermal therapy of orthotopic hepatocellular carcinoma. J. Mater. Chem. B 8, 4648–4659.
Xiao, Y., Ren, C., Chen, G., Shang, P., Song, X., You, G., Yan, S., Yao, Y., Zhou, H., 2022. Neutrophil membrane-mimicking nanodecoys with intrinsic anti-inflammatory properties alleviate sepsis-induced acute liver injury and lethality in a mouse endotoxemia model. Mate. Today Bio. 14, 100244.
Xie, S.-A., Zhang, T., Wang, J., Zhao, F., Zhang, Y.-P., Yao, W.-J., Hur, S.S., Yeh, Y.-T., Pang, W., Zheng, L.-S., 2018. Matrix stiffness determines the phenotype of vascular smooth muscle cell in vitro and in vivo: Role of DNA methyltransferase 1. Biomaterials 155, 203–216.
Xu, C., Pan, Y., Zhang, H., Sun, Y., Cao, Y., Qi, P., Li, M., Akakuru, O.U., He, L., Xiao, C., 2023. Platelet-Membrane-Coated Polydopamine Nanoparticles for neuroprotection by reducing oxidative stress and repairing damaged vessels in intracerebral hemorrhage. Adv. Healthc. Mater. 12, 2300797.
Yang, L., Wu, H., Liu, Y., Xia, Q., Yang, Y., Chen, N., Yang, M., Luo, R., Liu, G., Wang, Y., 2022. A robust mussel-inspired zwitterionic coating on biodegradable poly (L-lactide) stent with enhanced anticoagulant, anti-inflammatory, and anti-hyperplasia properties. Chem. Eng. J. 427, 130910.
Yao, Y., Wang, J., Cui, Y., Xu, R., Wang, Z., Zhang, J., Wang, K., Li, Y., Zhao, Q., Kong, D., 2014. Effect of sustained heparin release from PCL/chitosan hybrid small-diameter vascular grafts on anti-thrombogenic property and endothelialization. Acta Biomater. 10, 2739–2749.
Zhang, L., Yang, C., Song, Y., Sheng, T., Li, J., Yu, J., Wu, X., Ye, X., 2024. Advances of nanoparticles in transmucosal drug delivery. Nano Res. 17, 2874–2885.
Zhao, J., Fu, J.Y., Jia, F., Li, J., Yu, B., Huang, Y., Ren, K.F., Ji, J., Fu, G.S., 2023. Precise Regulation of Inflammation and Oxidative Stress by ROS-Responsive Prodrug Coated Balloon for Preventing Vascular Restenosis. Adv. Funct. Mater. 33, 2213993.
Zhao, Y., Xie, R., Yodsanit, N., Ye, M., Wang, Y., Wang, B., Guo, L.-W., Kent, K.C., Gong, S., 2021. Hydrogen peroxide-responsive platelet membrane-coated nanoparticles for thrombus therapy. Biomater. Sci. 9, 2696–2708.